



# Bulletin of the Mineral Research and Exploration

<http://bulletin.mta.gov.tr>



## APPLICATION OF TILT ANGLE METHOD TO THE BOUGUER GRAVITY DATA OF WESTERN ANATOLIA

Fikret DOĞRU<sup>a,b</sup>, Oya PAMUKÇU<sup>b\*</sup>, and İlkin ÖZSÖZ<sup>c</sup>

<sup>a</sup>Ataturk University, Oltu Earth Sciences Faculty, Department of Geophysics, Oltu, Erzurum [orcid.org/0000-0002-6973-1157](http://orcid.org/0000-0002-6973-1157)

<sup>b</sup>Dokuz Eylül University, Engineering Faculty, Geophysical Engineering, 35160, Buca, Izmir. [orcid.org/0000-0003-3564-1919](http://orcid.org/0000-0003-3564-1919)

<sup>c</sup>Dokuz Eylül University, Engineering Faculty, Geophysical Engineering, 35160, Buca, Izmir. [orcid.org/0000-0001-5907-4176](http://orcid.org/0000-0001-5907-4176)

Research Article

### Keywords:

Tilt angle, geological structural edges, Western Anatolia, Bouguer anomaly.

### ABSTRACT

In this study, tilt angle method was applied to Western Anatolia gravity data in order to estimate edges of the geological structures. Tilt angle was obtained in two different ways by using gravity and its vertical derivative. In potential field methods, tilt angle technique is expressed as the ratio of vertical derivative to horizontal derivatives of anomaly. In the tilt angle map, 0° contours defines structure edges, half of the distance between  $\pm 45^\circ$  defines depth of upper structure. In the field work of the study, gravity data, which was measured in Western Anatolia, was used to obtain regional anomaly maps and tilt angle and tilt angle of vertical directional derivative were applied to these maps. A significant difference was observed between western and eastern parts of the N-S striking line, throughout 28° longitude, from the results of tilt angle which was obtained by applying upward continuation method (50, 75 and 100 km) to the Bouguer anomaly. Same difference was determined from the results of vertical derivative of tilt angle which was obtained from upward continuation of Bouguer anomaly. Depth values were obtained from the results of tilt angle and vertical derivative of tilt angle methods between 7 and 43 km in study area. The obtained results were compared with geological structural boundary and possible depths of geological discontinuities were estimated. In addition, obtained results were investigated with seismic activity in the study area and compared with previous geological and geophysical studies.

Received Date: 21.06.2016

Accepted Date: 02.12.2016

## 1. Introduction

The general extent of fault-controlled Neogene basins occurring in Western Anatolia since Middle Miocene is NE-SW. The fillings which deposited during the Middle Miocene in these graben basins characterize generally fluvial, deltaic and lacustrine environments around Kütahya-Usak in the north and the lacustrine environment around Aydın-Denizli-Muğla regions in the south (Kaya, 1979; Leflef, 1980; Yılmaz, 2000). In other words, during this period fluvial systems developed roughly from north to south in many places and the lakes were located in the south and occasionally moved north. These NE-SW-trending graben basins, which contain fillings with ages reaching up to Middle Miocene to Pliocene and which are significant especially in the north of

Gediz Graben, have no genetic relationships with E-W and NW-SE stretching grabens resulting from K-G expansion (Hakyemez et al., 1999).

Extensive surfacing of the Early Quaternary fluvial sediments on the main active fault base block, which is located on the active south side of the graben, north of the main detachment fault and forming the boundary between the Holocene sediments and the Pleistocene sediments, probably indicates that the supra-detachment fault system over the fault of Gediz River basin filling axis in the late Pleistocene- early Holocene (in other words Gediz river bed) advanced towards the basin and as a result migrated towards the north (Hakyemez et al., 1999). Figure 1 shows a geology map of the study area and a map related to the location of the grabens.

\* Corresponding author: Oya PAMUKÇU, [oya.pamukcu@deu.edu.tr](mailto:oya.pamukcu@deu.edu.tr)  
<http://dx.doi.org/10.19111/bulletinmre.305177>

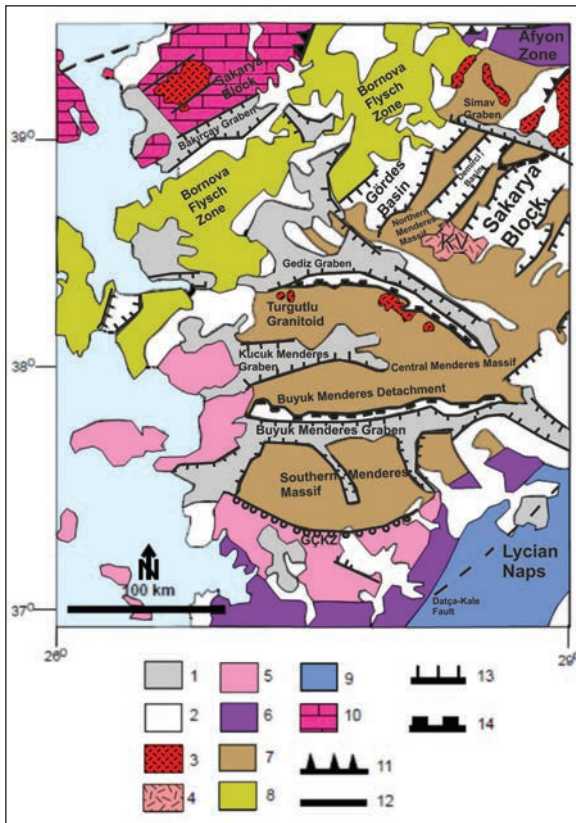


Figure 1- Geological map of Western Anatolia. Numbers are correspond to: 1: Alluvion, 2: Neogenevol-Volcano-Sedimentary Rocks, 3: Granite intrusions (Eocene-Miocene), 4: Alkaline Basalt Flow of Kula Volcanic Area (Upper Miocene-Quaternary), 5: Cycladic Complex (schist, marble, eclogite), 6: Afyon Zone metasedimanter and Pan-Afrikan basement rocks, 7: High-Grade Metamorphic Units of Menderes Core Complex (Precambrian-Senozoic), 8: Bornova Flysch and ophiolitic melange (Paleozoic-Paleocene), 9:Likya Naps and Tetis Ophiolits (Upper Cretaceous-Eocene), 10: Karakaya Complex (Permo-Trias) and Limestones (Jura-Upper Cretaceous), 11: Covergent boundary and major faults, 12: Continental minor strike slip faults, 13: Continental normal faults, 14: Detachment faults, KV: Kula Volcanites, GÇKZ: South Çine Shear Zone (It modified from Akay et al., 2013).

Determination of the boundaries of underground structures is very important in the modelling and mapping of geological structures. In geophysics, many methods are used to determine the boundaries of the anomaly-causing structure in potential methods. These methods are especially analytical signal (Roest et al., 1992), horizontal derivative, first and second vertical derivatives (Hood and Teskey, 1989; Roest et al., 1992), Euler deconvolution (Thompson, 1982; Blakely and Simpson, 1986, Pamukcu et al., 2007), Normalized Full Gradient (NFG) method (Pamukcu and Akcig, 2011), tilt angle map of vertical direction

derivative of gravity data (Oruç, 2011), which are used to reveal the boundaries of mass causing anomalies in gravity and magnetic methods. The arctangent of the ratio of the vertical derivative to the amplitude of total horizontal derivative gives the tilt angle. The comparison of tilt angle with horizontal derivative, second vertical derivative and analytical signal techniques was performed by Miller and Singh (1994). In this study, tilt angles of gravity anomaly and tilt angle values of the vertical derivative of anomaly were calculated and the results were interpreted. Tilt angle and tilt angle of the vertical derivative of anomaly methods were applied to the Bouguer gravity data of Western Anatolia and the geological structures in the area were examined.

During the field application phase of the study, tilt angle and tilt angle of vertical derivative methods were applied to the gravity data in the area where grabens in Western Anatolia are located. By using  $0^\circ$  and  $\pm 45^\circ$  contours in the tilt angle contour map, which was calculated at the end of the application, it is aimed to find possible geological structure boundaries and possible depths of the structures. Moreover, the anomalies created by the changes of the detected tilt values and the tectonic mechanisms defined in the study conducted by Gessner et al. (2013) have been compared. In Gessner et al. (2013) studies, it is seen that the region defined as Western Anatolia Transfer Zone (BATZ) is compatible with the findings obtained with the methods used in this study. In addition, the depth values found were compared with seismic activity and previous heat flux studies in the region and the results were found to be consistent.

## 2. Material and Method

The tilt angle in gravity is defined as the ratio of the vertical derivative of anomalies to the horizontal derivative. Mathematical expression of tilt angle;

$$\theta = \tan^{-1} \left( \frac{\frac{\partial^2 g_z}{\partial z^2}}{HGM} \right) \quad (1)$$

is defined as follows: Total horizontal component is defined as follows;

$$HGM = \left[ \left( \frac{\partial^2 g_x}{\partial x \partial z} \right)^2 + \left( \frac{\partial^2 g_y}{\partial y \partial z} \right)^2 \right]^{1/2} \quad (2)$$

In these equations, *HGM* shows total horizontal derivation;  $\theta$ , tilt angle;  $\frac{\partial^2 g_z}{\partial z^2}$ , the derivative of the Bouguer anomaly in the z direction;  $\frac{\partial^2 g_x}{\partial x \partial z}$ , the derivative of Bouguer anomaly in the x direction;  $\frac{\partial^2 g_y}{\partial y \partial z}$ , the derivative of Bouguer anomaly in the y direction.

The geometric meaning of the tilt angle is shown in figure 2.

An approach can be made about the depth of the source by the tilt angle contours. Tilt angle method's less sensitive to noise than other methods using higher order derivatives provides the commentator with a qualitative and quantitative perspective on the location and the depth, which is an important acquisition of the method (Akın et al., 2011).

$0^\circ$  value of the tilt angle gives the source limits. The half of the distance between the tilt angle contours ( $\pm 45^\circ$ ) gives the top depth of the structure (Salem et al., 2007; Oruç, 2011; Akın et al., 2011). The fact that the half-distance between the  $\pm 45^\circ$  contours in the gravity and magnetic tilt angle map does not show much change means that the structure depth does not show much change within itself.

### 3. Application

The study area is between  $36^\circ$  and  $40^\circ$  North latitudes,  $27^\circ$  and  $30^\circ$  East longitudes. The Bouguer gravity data collected by MTA (1979) in the studied area is overlaid on topographic data in figure 3. It is observed that the highest gravity value in the region is 90 mGal and the lowest value is -90 mGal. Figure 1 shows that the N-S stretch in the region is shown by normal faults. The grabens against N-S stretching are

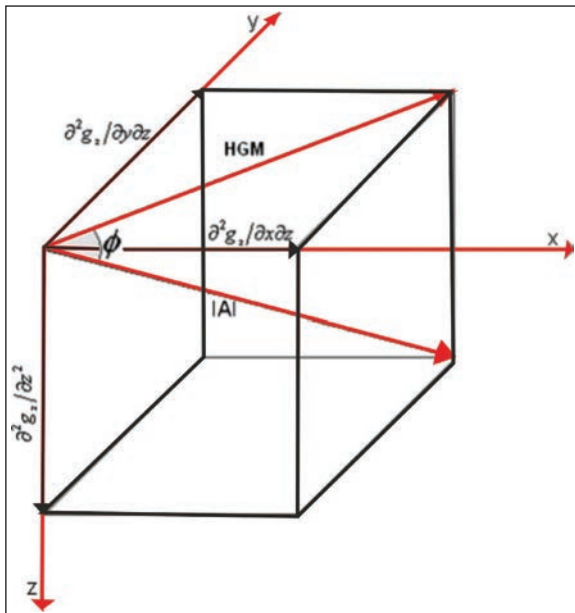


Figure 2- Geometrical representation of tilt angle for gravity method (It is modified from Oruç, 2011).

formed in E-W direction. Upwards analytical extension was applied on the Bouguer gravity anomaly of the study area and regional data were obtained (Figure 4).

The results of the tilt angle applied to figure 4 are shown in figure 5. Also, the results of the tilt angle applied after taking the vertical derivatives of figure 4 are shown in figure 6. It is observed that the results of the tilt angle method show the boundaries of the distinct geological structure in the region. The Menderes massif region in figure 1 corresponds to the low amplitude gravity anomaly seen in figure 4. The relative amplitude of anomaly rises towards the western Aegean Sea.

As mentioned earlier, half of the distance between the  $\pm 45^\circ$  contours provides information about the top depth of the structure. As a requirement of the method, the sections were selected in the places where the  $\pm 45^\circ$  contours were placed. In particular, to study the depth values in the north and south of the study area, the distances between the contours of  $\pm 45^\circ$  were determined by taking the slices using the maps in figures 5 and 6, and the obtained results are given in figures 7-8. The depths found as a result of the calculations made in the sections taken in figures 7-8, are given in table 1.

Gessner et al. (2013) suggested that a shear zone was formed as a result of the tectonic erosion formed in the Menderes Massif by the subduction zone defined in the Aegean region and Decomposition in the lithospheric mantle beneath the continent and they defined it as Western Anatolia Transfer Zone. The Western Anatolia Transfer Zone defines the lateral boundary between the Hellenide and Anatolide orogenies. The Anatolian Transfer Zone has a transtensional structure which is the result of the erosion of the Menderes Massif in Miocene with extensive lithospheric stress (Gessner et al., 2013). Figures 6c, 6d and 6e show an N-S stretch between  $27^\circ$  and  $28^\circ$  east longitudes. This structure is defined as Western Anatolia Transfer Zone (WATZ) by Gessner et al. (2013).

The tilt angle change maps are shown in in figures 6c, 6d, and 6e, which are determined in this study, and approximate boundaries of WATZ as defined by Gessner et al. (2013) are given in figure 9. According to Gessner et al. (2013), it is seen that the marked WATZ is compatible with the N-S striking structure between the  $27^\circ$  and  $28^\circ$  east longitudes in figures 9a, 9b and 9c.

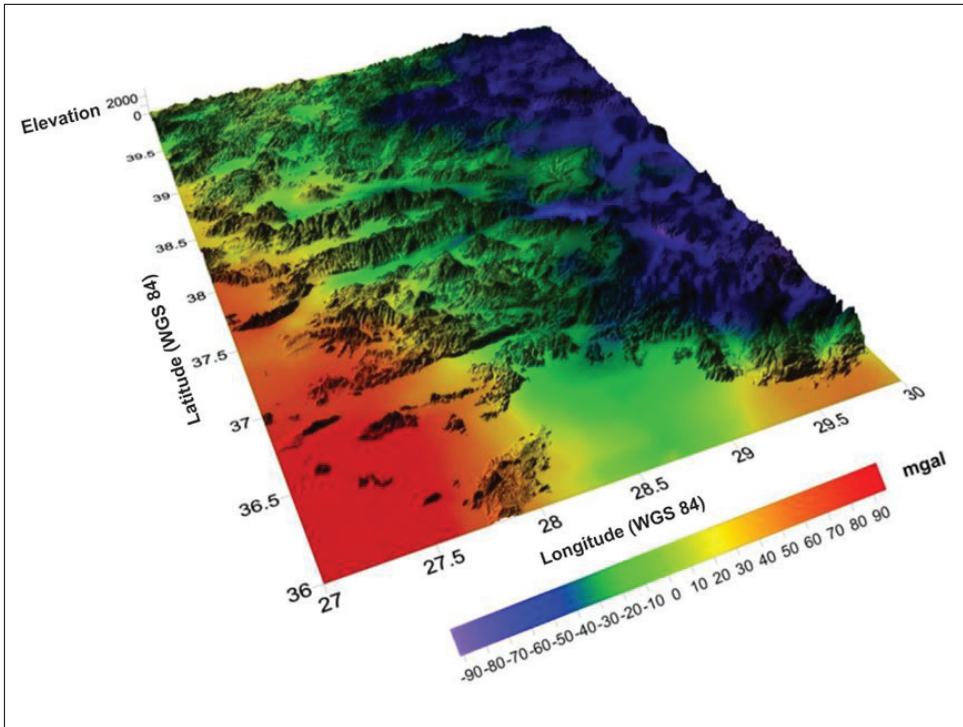


Figure 3- Bouguer gravity anomaly map illustrated on topography of study area.

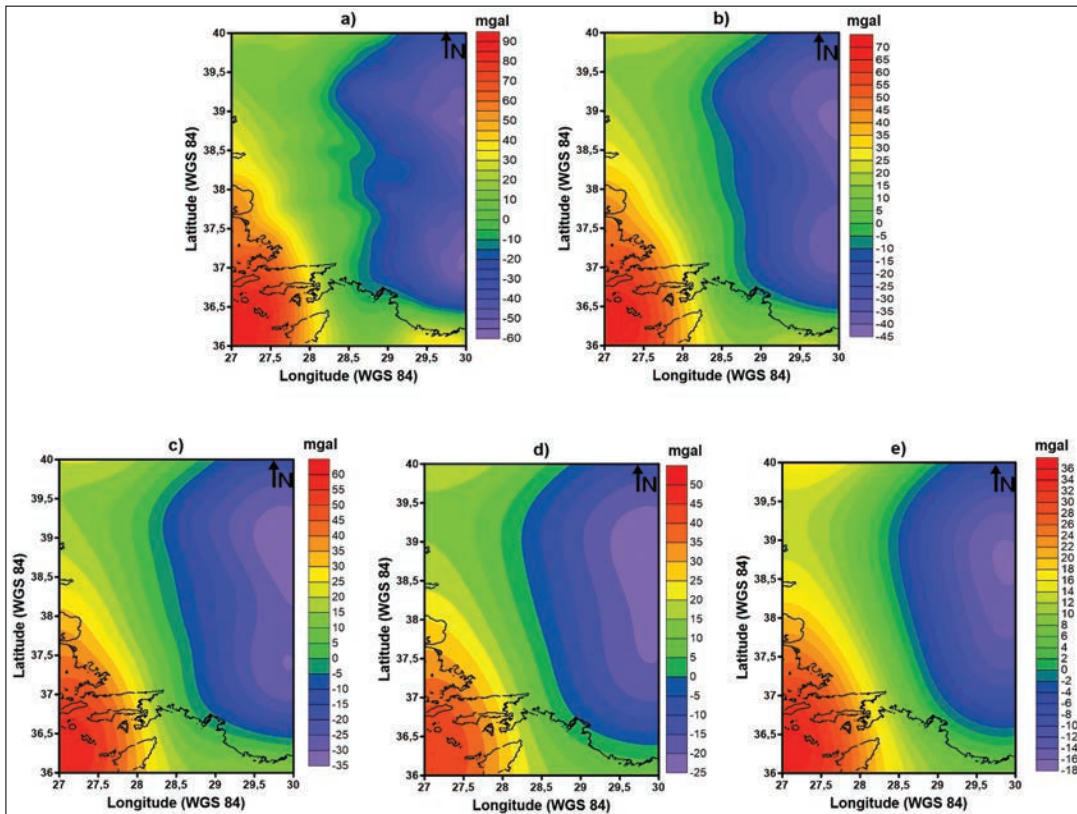


Figure 4- Regional data having different upward continuation values in study area: a) Continuation plane is 15 km, b) 35 km, c) 50 km, d) 75 km and e) 100 km (Black line illustrates coastal boundaries).

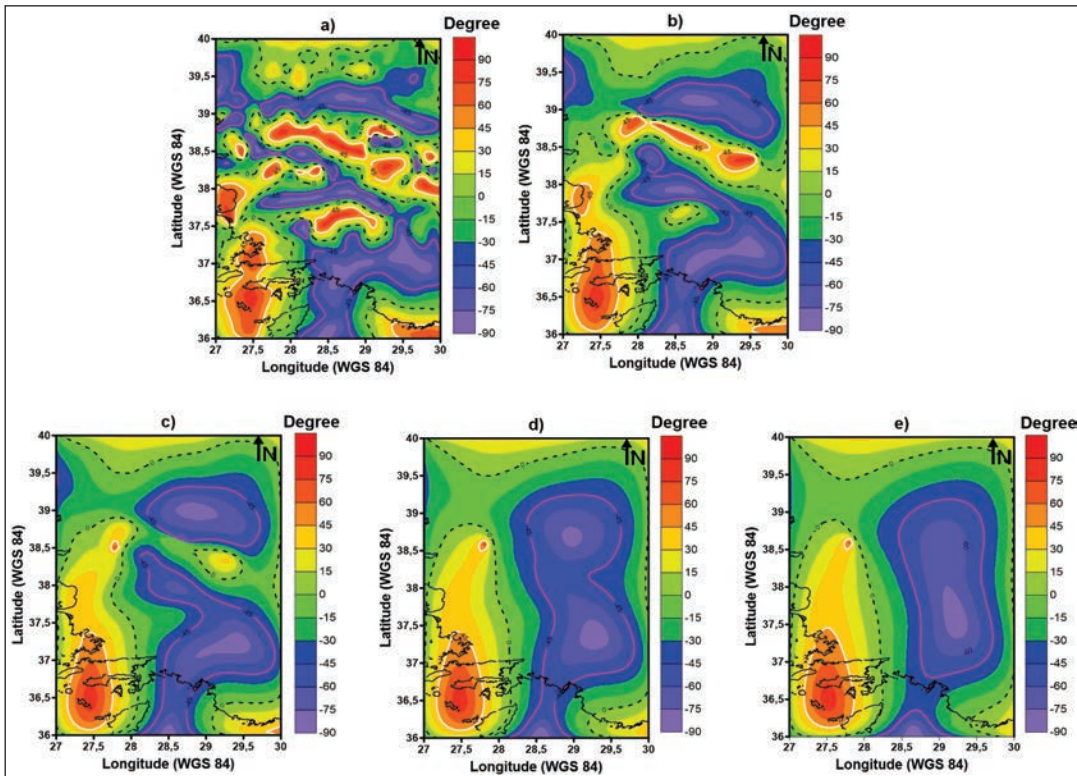


Figure 5- Tilt angle results of regional data having different upward continuation values: a) Continuation plane is 15 km, b) 35 km, c) 50 km, d) 75 km, e) 100 km (Contours are illustrated following, White +45°, Pink -45° and black dashed lines 0°).

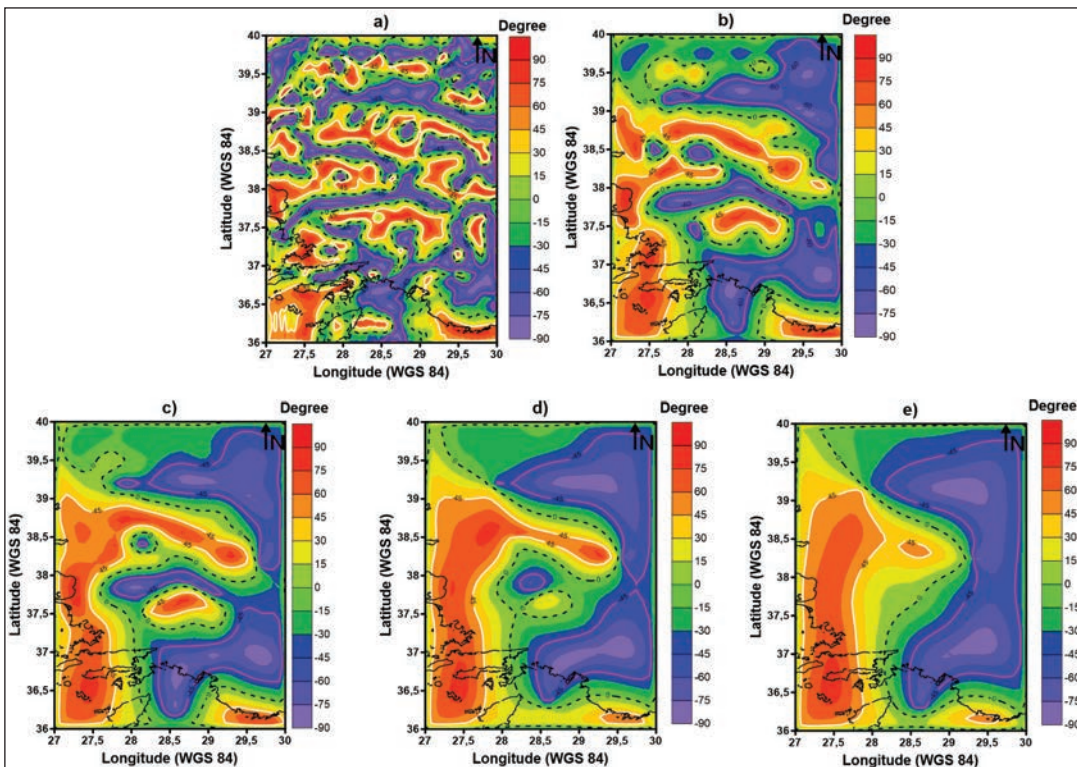


Figure 6- Tilt angle results of vertical derivative of regional data having different upward continuation values: a) Continuation plane is 15 km, b) 35 km, c) 50 km, d) 75 km, e) 100 km (Contours are illustrated following, White +45°, Pink -45° and black dashed lines 0°).

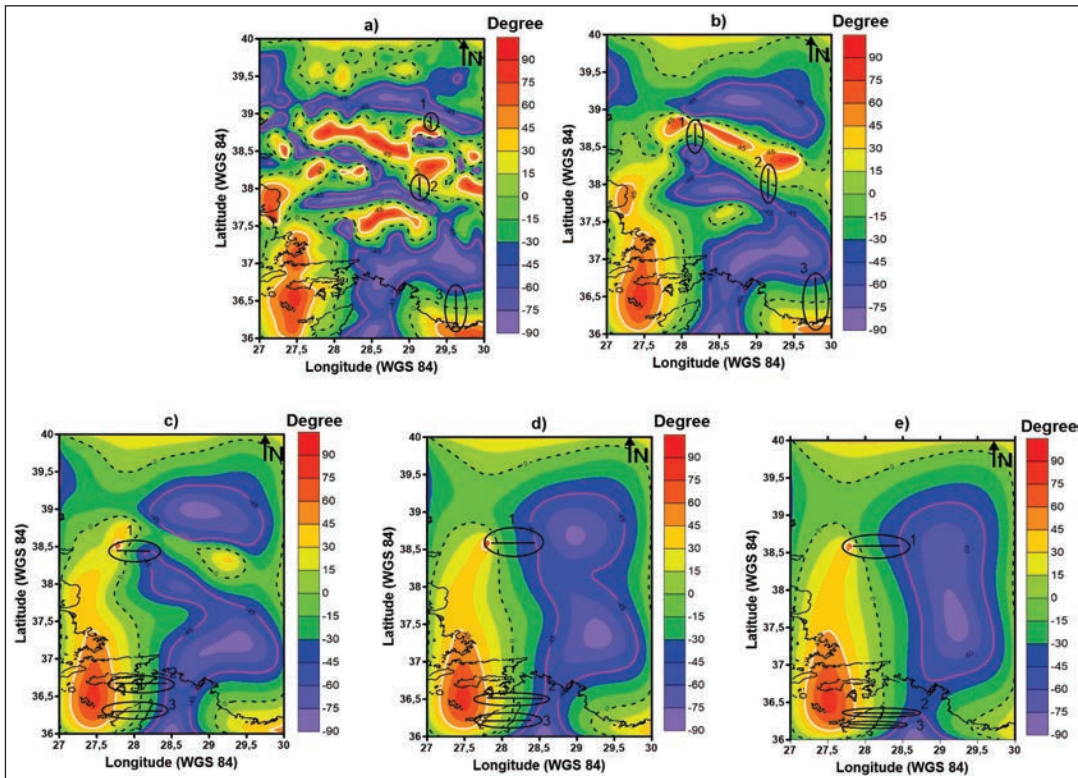


Figure 7- Sections are shown in ellipses which illustrate depth estimation of regional data having different upward continuation values using tilt angle method: a) Continuation plane is 15 km, b) 35 km, c) 50 km, d) 75 km, e) 100 km.

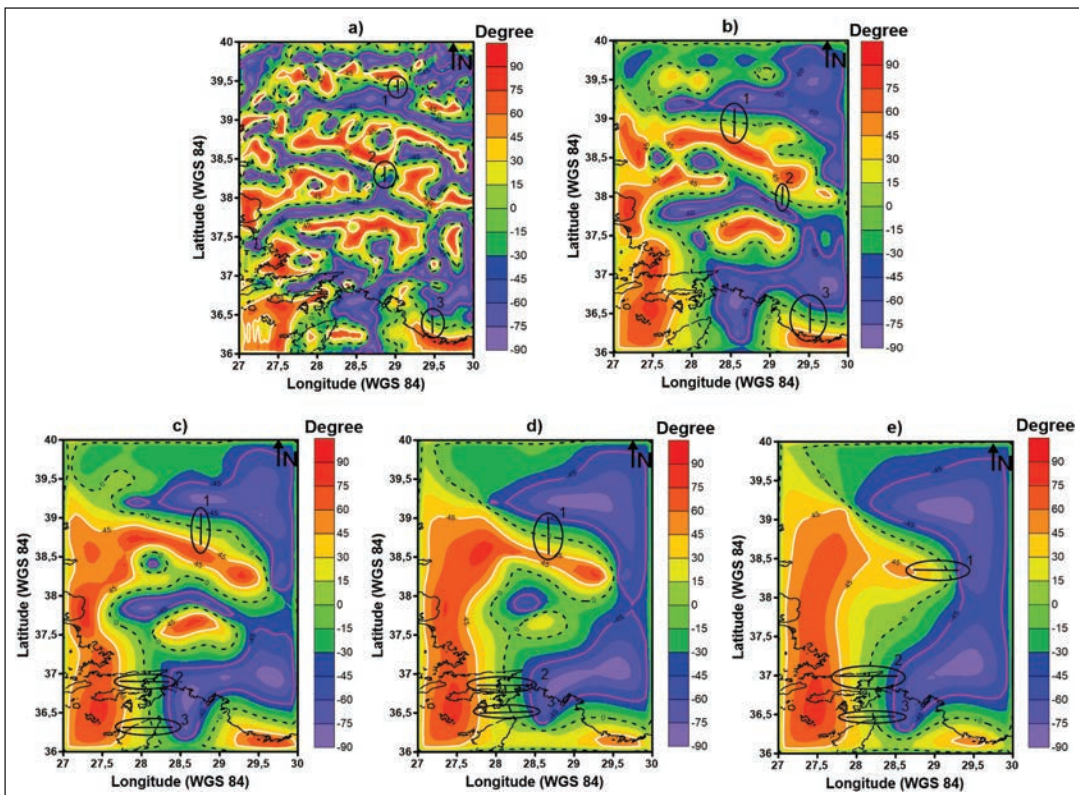


Figure 8- Sections are shown in ellipses which illustrate depth estimation of vertical derivative of regional data having different upward continuation values using tilt angle method: a) Continuation plane is 15 km, b) 35 km, c) 50 km, d) 75 km, e) 100 km.

Table 1- Top depths are obtained from tilt angle method and tilt angle of vertical derivative of anomaly.

Data	Depths are Obtained from Tilt Angle Method			Depths are Obtained from Tilt Angle of Vertical Derivative of Anomaly			Averages		
	Section 1 (km)	Section 2 (km)	Section 3 (km)	Section 1 (km)	Section 2 (km)	Section 3 (km)	Section 1 (km)	Section 2 (km)	Section 3 (km)
Continuation Plane 15 km	7.78	13.55	25.14	7.16	10.33	12.55	7.47	11.94	18.84
Continuation Plane 35 km	17.28	21.66	33.33	13.27	13.50	20	15.27	17.58	26.66
Continuation Plane 50 km	23.88	39.44	36.66	23.33	34.99	34.88	23.61	37.21	35.77
Continuation Plane 75 km	31.63	41.1	36.10	24.16	35.83	37.61	27.89	38.46	36.85
Continuation Plane 100 km	33.88	43.84	37.20	31.66	41.00	34.44	32.77	42.42	34.98

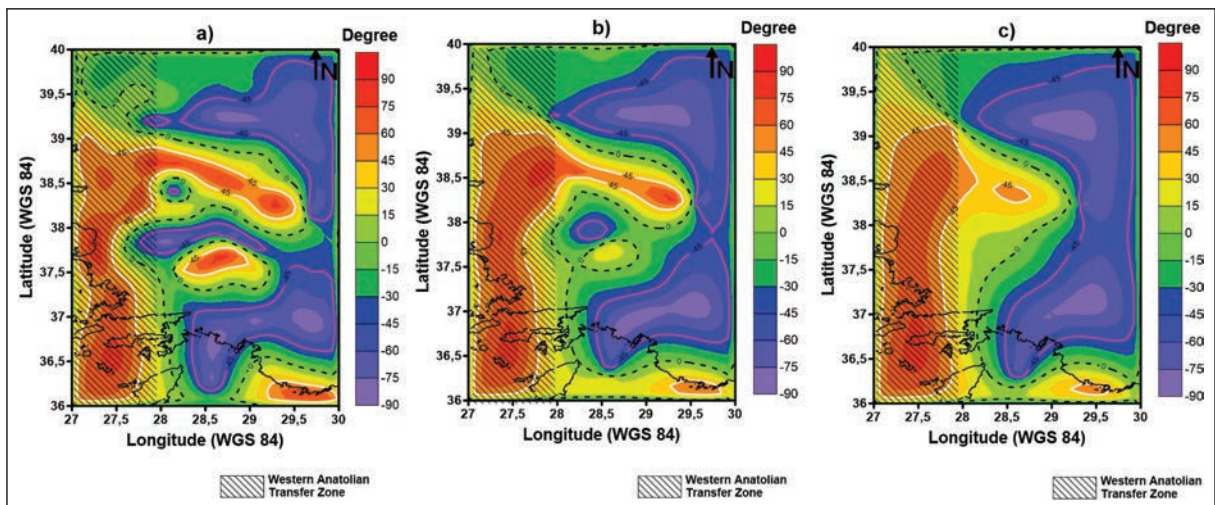


Figure 9- Boundary of Western Anatolian Transfer Zone. Western anatolian Transfer Zone illustrated on regional datas that are: a) Continuation plane is 50 km, b) 75 km, c) 100 km.

In order to approach the possible structure depth, the depths of the tilt angle data and averages of the depths were found at the tilt angle of the vertical derivative. As can be seen, the average of the sections 1, 2 and 3 from the data with the extension plane of 50 km gave similar depths. Also, the  $\pm 45^\circ$  contours of the data in which tilt angle is taken from the vertical derivative showed less variation than the  $\pm 45^\circ$  contours obtained from the tilt angle. The sections were first taken from the tilt map of the vertical derivative and then taken from the tilt angle map, corresponding to approximately the same latitude.

The average crustal thickness is 26 km deep in the eastern part of WATZ, according to tilt angle result, considering section 1 values of the results of the upward extension of 35, 50 and 75 km in table 1. At the same time, looking at the upwards extension values in this region, a sudden decrease in gravity value was

observed. According to Şalk et. al (2005) it is observed that the values of the heat flux obtained by using Curie depths calculated from magnetic data are increased. In addition, it is observed that there is a passive zone in terms of producing earthquakes here, considering the earthquakes with 3.5 or above magnitude were taken from the USGS earthquake catalogue. The heat fluxes obtained by using the magnitudes and depths of the earthquakes in the region and the Curie depths calculated from the magnetic data are associated with each other and they are shown in figure 10 (Şalk et al., 2005).

As can be seen from figure 10; in regional data, between  $28.5^\circ$  and  $29.5^\circ$  East longitudes and between  $38^\circ$  and  $39^\circ$  North latitudes, the number of earthquakes is small and they are in shallow depths. When we look at the heat flux maps obtained using the Curie depths calculated from magnetic data, there is a zone where

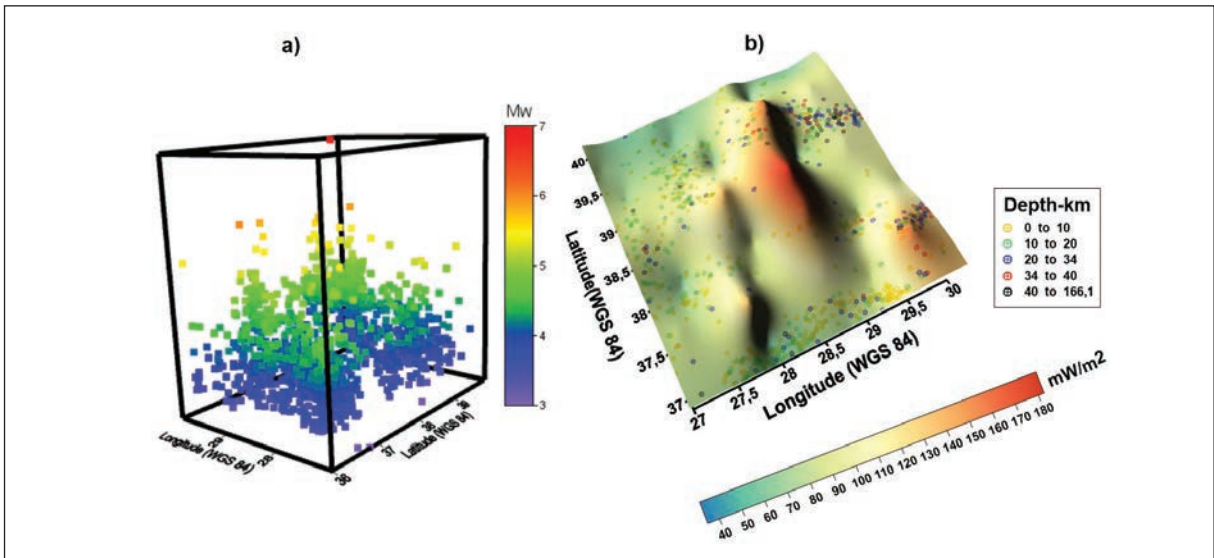


Figure 10- Examination of Earthquakes and heat flow maps that obtained from Curie depths in study area: a) Earthquakes in study area is showed latitude, longitude and magnitude, b) Examination of earthquake depths and heat flow map for study area. (Earthquake data is downloaded from USGS).

the heat flux is increased in the same region between 28.5° and 29.5° East longitudes, 38° and 39° North latitudes.

The earthquake depth relation graph is shown in figure 11. As a result of the earthquake analysis made in the study area, it is observed that the number of earthquakes decreased significantly between 34 and 200 km depths. Especially in isostatic studies, such environments are considered as the transition from a rigid environment to a ductile environment (Watts,

2001; Pamukcu and Yurdakul, 2008; Pamukcu and Akçığ, 2011). As can be understood from this chart, there is a decrease of about 50% in the number of earthquakes at 34 km. This decrease in the number of earthquakes corresponds to the area of the third section of the observed area, 35 km upwards extension and 50 km upwards extension (Table 1). When compared to the change of the heat flux values determined by Şalk et al (2005); regions with high heat flux were observed to be related to this field (Figure 10).

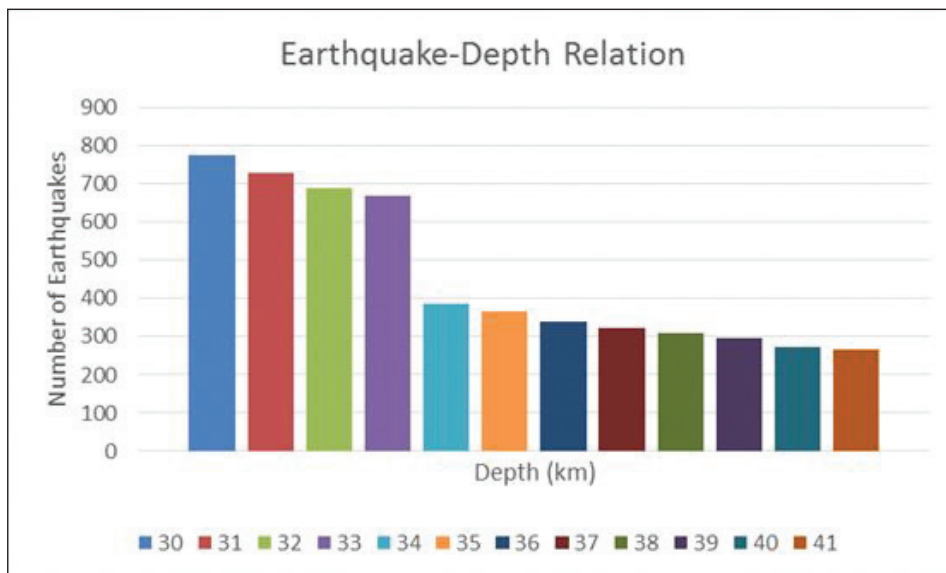


Figure 11- Relationship between number and depth of earthquakes. (<https://www.usgs.gov/>).



#### 4. Results

In this study, the results obtained by applying the tilt angle method to the land gravity data have been examined. In addition, tilt angle method was applied to the vertical derivatives of terrain data using the approach in Oruç's study (2011).

The upper depths found by using tilt angle for western Anatolia were compatible with the depths in the studies conducted by Çifçi et al. (2011), Pamukcu and Yurdakul (2008) using seismology, gravity and seismic data in the same region. The average depths obtained for the various upward extension planes in table 2 are compatible with depths of crustal corrugations determined by seismic reflection evaluation by Çifçi et al. (2011). Depths determined in applications after 50 km of extension plane and the upper depth of deep structure controlling the anomaly were determined to change in the north- east direction between 30 and 40 km in the Western Anatolia Region (Table 2). This result is consistent with the crustal thickness value determined by Zhu et al. (2006).

Depths and boundaries obtained from the tilt angle of the vertical derivative method in field study are quite compatible with boundaries of the lithospheric zone offered for the Western Anatolia Region by Gessner et al. (2013). This lithospheric zone, which is also observed by the tilt angle method, is thought to be caused by the progression of the hot material formed by subduction zone defined by Gessner et al. (2013) in the part where the number of earthquakes is small to the upper part of the lithosphere and making the environment ductile. A decrease in the number and depth of earthquakes is seen as a result of being ductile (Figure 11) and the heat flux values in the same region are observed to rise (Figure 10b). In this study, it was found that the upper depth of zone from tilt values changed between 18 and 38 km from table 1.

In this study, two approaches can be mentioned by looking at the  $0^\circ$  and  $\pm 45^\circ$  contours in the anomalies in figures 9a, 9b and 9c. In the first approach, there are two different geological structures extending from north to south. In the second approach, there is a single structure here, but the structure remaining in the east underwent deformation. The second approach was also mentioned in the study conducted by Gessner et al. (2013).

When the earthquake quantities and depths in the study area are analyzed together (Figure 11), it can

be said that there is a fragile environment up to 34 km in the region and after 34 km, the transition to the ductile environment begins. When the regional maps in figure 4 are examined, it can be observed that the Bouguer anomaly is low in the east of the study area and it is also observed that the values of the heat flux obtained by using Curie depths calculated from the magnetic data in the east of the field increase. These characteristics indicate a ductile environment, but the Bouguer anomaly is high at the west of the field (Figure 4) and the heat flux values obtained using Curie depths calculated from magnetic data are low (Figure 10b). As a result, the western part, which is determined from the tilt angle change and is defined as the Western Anatolian Transfer Zone by Gessner et al. (2013), may still be a rigid structure even at a depth of about 34 km.

#### Acknowledgement

We would like to thank Prof. Dr. Bülent Oruç, who shared his valuable opinions in the evaluation of the article and the two reviewers.

#### References

- Akay, T., Bilim F., Koşaroğlu, S. 2013. Menderes Masifi tektonik yapılarının (Batı Anadolu, Türkiye) Bouguer gravite analizi kullanılarak incelenmesi. Cumhuriyet Yerbilimleri Dergisi, 30, 2, 71-86.
- Akın, U., Şerifoğlu, B.I., Duru, M. 2011. Using the tilt angle in gravity and magnetic methods. Bulletin of the Mineral Research and Exploration, 143, 1-12.
- Blakely, R.J., Simpson, R.W. 1986. Approximating edges of source bodies from magnetic or gravity anomalies. Geophysics, 51(7), 1494-1498.
- Çifçi, G., Pamukcu, O., Çoruh, C., Çopur, S., Sözbilir, H. 2011. Shallow and deep structure of a supradetachment basin based on geological, conventional deep seismic reflection sections and gravity data in the Buyuk Menderes Graben, western Anatolia. Surveys in Geophysics, 32(3), 271-290.
- Gessner, K., Gallardo, L.A., Markwitz, V., Ring, U., Thomson, S.N. 2013. What caused the denudation of the Menderes Massif: Review of crustal evolution, lithosphere structure, and dynamic topography in southwest Turkey. Gondwana Research, 24(1), 243-274.
- Hakyemez, H.Y., Erkal, T., Göktaş, F. 1999. Late Quaternary evolution of the Gediz and Büyük menderes

- grabens, western Anatolia, Turkey. *Quaternary Science Reviews*, 18(4), 549-554.
- Hood, P.J., Teskey, D.J. 1989. Aeromagnetic gradiometer program of the geological survey of Canada. *Geophysics*, 54(8), 1012-1022.
- Kaya, O., 1979. Ortadoğu Ege çöküntüsünün (Neojen) stratigrafisi ve tektoniği. *Türkiye Jeoloji Kurumu Bült.*, 22, 35-58.
- Leflef, D., 1980. Muratdağı güneyi Neojen havzasının çökel ortamları ve paleocoğrafik evrimi. Maden Tetkik ve Arama Genel Müdürlüğü Raporu No: 6812, Ankara (unpublished).
- Maden Tetkik ve Arama Genel Müdürlüğü (MTA) 1979. Batı Anadolu Bouguer gravite haritası (unpublished).
- Miller, H.G., Singh, V. 1994. Potential field tilt—a new concept for location of potential field sources. *Journal of Applied Geophysics*, 32(2), 213-217.
- Oruç, B. 2011. Edge detection and depth estimation using a tilt angle map from gravity gradient data of the Kozaklı-Central Anatolia region, Turkey. *Pure and applied geophysics*, 168, 10, 1769-1780.
- Pamukcu, O. A., Akçığ, Z., Demirbaş, Ş., Zor, E. 2007. Investigation of crustal thickness in Eastern Anatolia using gravity, magnetic and topographic data. *Pure and Applied Geophysics*, 164, 11, 2345-2358.
- Pamukcu, O. A., Yurdakul, A. 2008. Isostatic compensation in western Anatolia with estimate of the effective elastic thickness. *Turkish Journal of Earth Sciences*, 17, 3, 545-557.
- Pamukcu, O. A., Akçığ, Z. 2011. Isostasy of the Eastern Anatolia (Turkey) and discontinuities of its crust. *Pure and applied geophysics*, 168, 5, 901-917.
- Roest, W.R., Verhoef, J., Pilkington, M. 1992. Magnetic interpretation using the 3-D analytic signal. *Geophysics* 57, 1, 116-125.
- Salem, A., Williams, S., Fairhead, D., Smith, R., Ravat, D. 2007. Interpretation of magnetic data using tilt-angle derivatives. *Geophysics*, 73, 1, L1-L10.
- Şalk, M., Pamukcu, O., Kaftan, I. 2005. Determination of the Curie point depth and heat flow from MAGSAT data of Western Anatolia. *Journal of the Balkan Geophysical Society*, 8, 4, 149-160.
- The United States Geological Survey (USGS) Earthquake hazards program, URL: <http://earthquake.usgs.gov/>.
- Thompson, D.T. 1982. EULDPH: A new technique for making computer-assisted depth estimates from magnetic data. *Geophysics*, 47, 1, 31-37.
- Watts, A. B. 2001. *Isostasy and Flexure of the Lithosphere*. Cambridge University Press.
- Yılmaz, Y. 2000. Ege Bölgesinin aktif tektoniği. Batı Anadolu'nun depremselliği Sempozyumu (BADSEM 2000), 24-27 Mayıs 2000, İzmir, Bildiriler, 3-14.
- Zhu, L., Mitchell, B. J., Akyol, N., Cemen, I., Kekovali, K. 2006. Crustal thickness variations in the Aegean region and implications for the extension of continental crust. *Journal of Geophysical Research: Solid Earth*, 111(B1).